THE JOURNAL OF PHYSICAL CHEMISTRY C
A JOURNAL OF THE AMERICAN CHEMICAL SOCIETY

pubs.acs.org/JPCC

Article

Efficient Photothermal Generation by Nanoscale Light Trapping in a Forest of Silicon Nanowires

Antonio Ferraro, Pino Cerza, Valentina Mussi, Luca Maiolo, Annalisa Convertino,* and Roberto Caputo*

Cite This: *J. Phys. Chem. C* 2021, 125, 14134−14140

Read Online

ACCESS | Metrics & More | Article Recommendations | Supporting Information

ABSTRACT: We experimentally investigate the photothermal conversion in disordered silicon nanowires (SiNWs) grown on a glass substrate by plasma-enhanced chemical vapor deposition. The temporal and spatial response under illumination of a 532 nm laser has been measured by means of an infrared (IR) thermocamera. Fast heat generation and adjustable temperature increase from a few tens up to ≈600 °C have been observed in a confined small region around the laser spot. The performing photothermal conversion is related to the efficient light trapping in SiNWs, providing enhanced absorption in the visible spectrum, and nonradiative recombination of the photogenerated carriers, typically occurring in Si. These findings combined with a low-cost, low-temperature, and large-area fabrication technology promote the disordered SiNWs as a flexible heat source well suited for applications in multiple fields including biology, precision medicine, gas detection, and nanometallurgy.

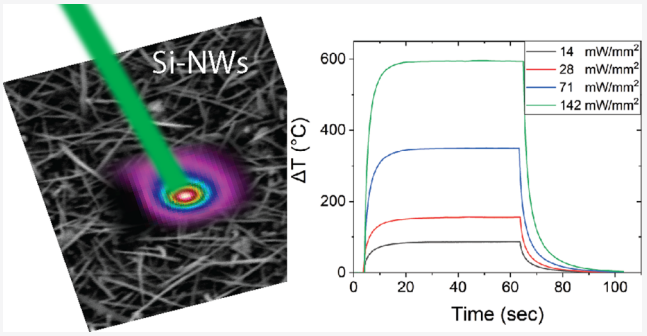

INTRODUCTION

Nanostructures have found remarkable interest since they represent a bridge between a macroscopic and an atomic structure, with fascinating and tailorable properties, suitable for a wide range of applications in the fields of energy, lighting, molecular medicine, and life science, to name a few.[1−5] Recently, the fine control of the heat generation in photothermal nanomaterials is gaining much attention[6−15] due to their promising applications in cancer treatment[16] and in the direct collection, conversion, and storage of solar radiation as thermal energy.[17] In fact, under the action of a laser beam or sunlight, a photothermal nanostructure, consisting generally of metal or semiconductor nanoparticles, exhibits a high absorption of light, effectively transforming itself into an ideal nanosource of heat remotely controllable by light. The control of temperature on the nano−microscale using nanomaterials, with photothermal peculiar properties, have a much broader application range since several temperature-mediated processes in biology and chemistry can be opportunely tuned and controlled. For example, different biochemical reactions occurring in individual cells, like an ion channel function,[18−20] cellular stimulation,[21−23] and heat shock protein expression,[24] are extremely sensitive to temperature variations. Therefore, delivering a thermal stimulus in the range of 35−45 °C directly and precisely to a region of micron and submicron dimensions will allow investigating cellular processes mediated by temperature with almost single-cell resolution or to realize novel therapeutic applications requiring a selective thermal stimulation.[25] Another interesting field of application is the detection of gases using conductive metal oxide sensors, which are one of the most relevant classes of gas sensors. The gas sensing process is strongly related to surface reactions, influenced by several factors including the working temperature,[26] which typically ranges between 200 °C and 400 °C. Thus, coupling a micro−nanoheater to metal oxide sensing materials could offer the remarkable advantage of fabricating a large array of chemically different sensing elements, which can be operated independently, having fast response and remote control (i.e., programmable in the order of milliseconds) supported by the implementation of thermal schedules.[27] These features are particularly convenient when the sensor array is conceived as an "electronic nose" since the individual sensing elements possess unique temperature programs and material coatings due to variations in surface processes. The above mentioned examples indicate that diverse applications require specific ranges of operation temperature that can differ by a few orders of magnitude. However, a single nanostructure meeting the requirements of multiple photothermal applications is still a challenge. Here, we report on the extraordinary

Received: April 26, 2021
Revised: June 9, 2021
Published: June 17, 2021

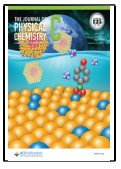

https://doi.org/10.1021/acs.jpcc.1c03732
J. Phys. Chem. C 2021, 125, 14134−14140

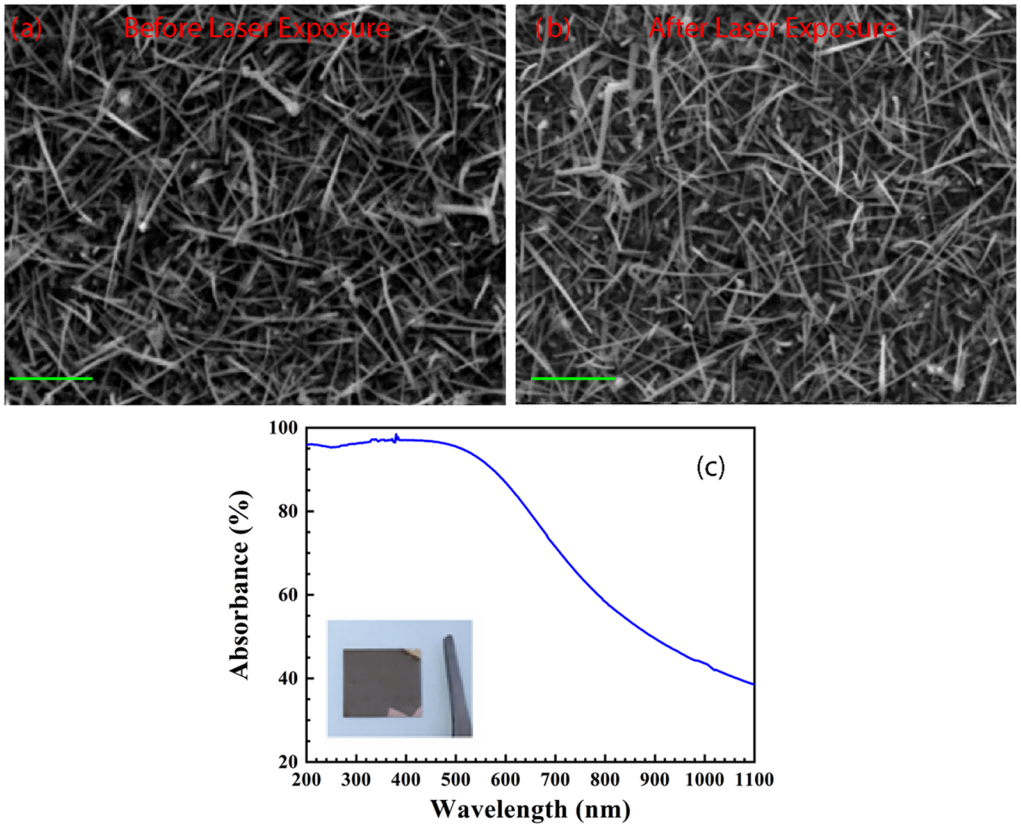

Figure 1. Scanning electron microscope (SEM) micrographs of the fabricated silicon nanowires (SiNWs) before (a) and after (b) exposure to the 532 nm CW laser at an intensity of 142 mW/mm^2 for 60 s; scale bar 1 μm. (c) Optical absorbance spectrum of SiNWs on a microscope glass; image is shown in the inset.

photothermal properties of randomly arranged and oriented silicon nanowires (SiNWs), which can rapidly deliver a laser-controlled thermal stimulus in a very wide operation range ranging from a few to ≈600 °C. In particular, we investigate the photothermal conversion capability of SiNWs, 2−3 μm long with an average diameter of 40−60 nm, grown by plasma-enhanced chemical vapor deposition (PECVD) on a glass substrate. These materials have been recently demonstrated to be very versatile since they can promote interaction with micro/nanoscale features of mammalian cells[28,29] and allow a facile detection of biomolecules[30−33] and gases.[34] By leveraging efficient light trapping[35,36] with nonradiative carrier recombination,[37] a SiNW forest generates in a few seconds a photothermal response to a green continuous-wave (CW) laser irradiation as recorded by an infrared (IR) thermocamera. In particular, the photothermal heat released from the SiNWs can be controlled continuously between room temperature and ≈600 °C, depending on the laser power, with high spatial confinement. To characterize the transient temperature change, the intensity of the laser beam was modulated using a chopper at frequencies of 1, 5, and 10 Hz. The local temperature of the SiNWs changes differently depending on the modulation frequency, and the measured increments are in all cases lower with respect to the static condition due to the limited time available to reach the maximum temperature. However, it is possible to reach a significant ΔT of 150 °C in a period. These findings suggest that SiNWs can effectively deliver a temporally and spatially modulated thermal stimulus controlled by a laser signal. By considering that the disordered arrangement of SiNWs offers the key technological benefit of using bottom-up fabrication technologies at low growth temperatures, compatible with some polymeric film such as polyimide and glassy supports,[30,38,39] these photoabsorbing structures can be readily combined with high spatio-temporal resolution projection systems, including commercial spatial light modulators (SLMs) for generating computer-controlled holographic patterns. This will pave the way toward new tools suited for holographically controlled photothermal excitation by allowing parallel stimulation of multiple points at tunable local light intensities with time modulation. We envision that the proposed platform will stimulate novel temperature-controlled applications ranging from a new technology for computer-controlled thermal stimulation of neuronal tissue[24] and minimally invasive surgical laser-guided tools for photothermal treatment of tumors[40] to microheaters or microhotplates whose working principle will be based on photothermal conversion instead of the Joule heating effect.

METHODS

Nanofabrication. Au-catalyzed SiNWs were produced by plasma-enhanced chemical vapor deposition (PECVD) on microscope glass slides. To induce the NW growth, a 2 nm thick Au film was evaporated on a substrate. The SiNW growth was performed with SiH_4 and H_2 as precursors, at a total pressure of 1 Torr and the flow ratio $SiH_4/(H_2 + SiH_4)$ fixed to 1:10. The substrate temperature was kept at 350 °C. A 13.6 MHz radiofrequency with power fixed at 5 W was used to ignite the plasma.

Scanning Electron Microscope (SEM). The morphology of the SNWs was verified by scanning electron microscopy

https://doi.org/10.1021/acs.jpcc.1c03732
J. Phys. Chem. C 2021, 125, 14134−14140

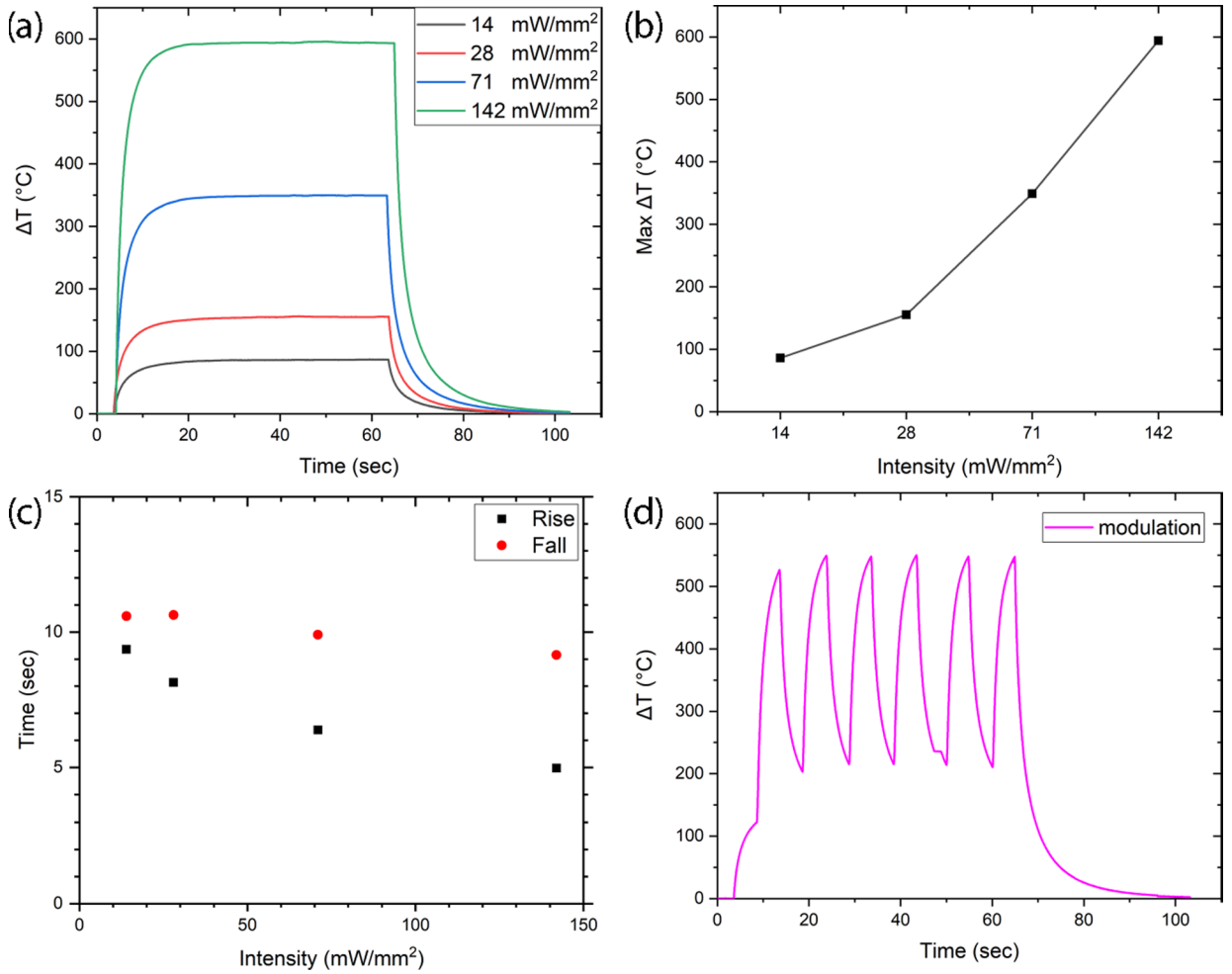

Figure 2. (a) Experimental macroscopic temperature variation (ΔT) at different laser intensities (λ = 532 nm) for the proposed SiNWs, (b) maximum temperature variation (ΔT) as a function of the laser intensity, (c) rise (10−90) and decay (90−10) time for SiNWs as a function of the laser intensity, and (d) experimental macroscopic temperature where every 10 s the intensity is changed from 28 to 142 mW/mm^2.

(SEM). A ZEISS EVO MA10 SEM was used at an accelerating voltage of 5 kV. The size of the NWs was determined by combined measurements from top and cross-sectional views and using line tools of the image analysis program ImageJ

Thermal Measurement. For macroscopic thermal measurement, a COHERENT Verdi λ = 532 nm CW laser was used as a source. A pinhole with a diameter of 3 mm was used to reduce the beam spot. The macroscopic thermal measurement was acquired using an IR camera FLIR E40 having an IR resolution of 160 × 120 pixel, a spatial resolution (IFOV) of 2.72 mrad/pixel, and maximum acquired temperature of 650 °C. The emissivity, experimentally retrieved, was fixed at 0.97. The measurement was started 3 s prior the beam impinged on the sample for 60 s. Then, the beam was shut off and the temperature decay was measured for 40 s. For dynamic thermal measurement, a chopper, with an adjustable frequency, was interposed between the laser source and the sample.

RESULTS AND DISCUSSION

Morphological and Optical Characterization of the SiNWs. Figure 1a shows the scanning electron microscopy (SEM) image of the SiNWs grown on a microscope glass; a representative image of the full-scale sample is instead reported in the inset of Figure 1c. The structure consists of a forest of disordered and randomly oriented SiNWs, around 2−3 μm long, with a tapered shape and an average diameter at the bottom of about 40−60 nm. Since the photothermal response was investigated by exposing the sample to a green CW laser with λ = 532 nm, at different laser intensities, in the range 14−142 mW/mm^2, we studied the effect of laser irradiation on the morphology of the SiNWs. Figure 1b shows the SEM image of the SiNWs after exposure to the maximum laser intensity of 142 mW/mm^2 for 60 s. By comparing the SEM images in Figure 1, no evident change in the morphology of the NWs is noticeable after laser irradiation, confirming their high mechanical and thermal resistance. Before performing the photothermal experiments, the optical behavior of the SiNWs was investigated in terms of reflectivity, R, and transmissivity, T, in the spectral range between 200 and 1100 nm. The calculated absorbance, $A = 100 - R - T$, plotted in Figure 1c, shows a strong light absorption in the whole UV−vis spectral range. This is due to the multiple scattering events that the light undergoes by interacting with NWs while passing through structures like those in Figure 1a or b. The multiple scattering folds the light path many times in a random walk within the forest, thus causing an enhancement of light absorption at the frequencies absorbed by the NW material, i.e., light trapping.[35,36] It is worth noting that the increase of the absorption starts at 1100 nm, which corresponds to the band gap (1.12 eV) of crystalline Si (c-Si), and increases its slope for

https://doi.org/10.1021/acs.jpcc.1c03732
J. Phys. Chem. C 2021, 125, 14134−14140

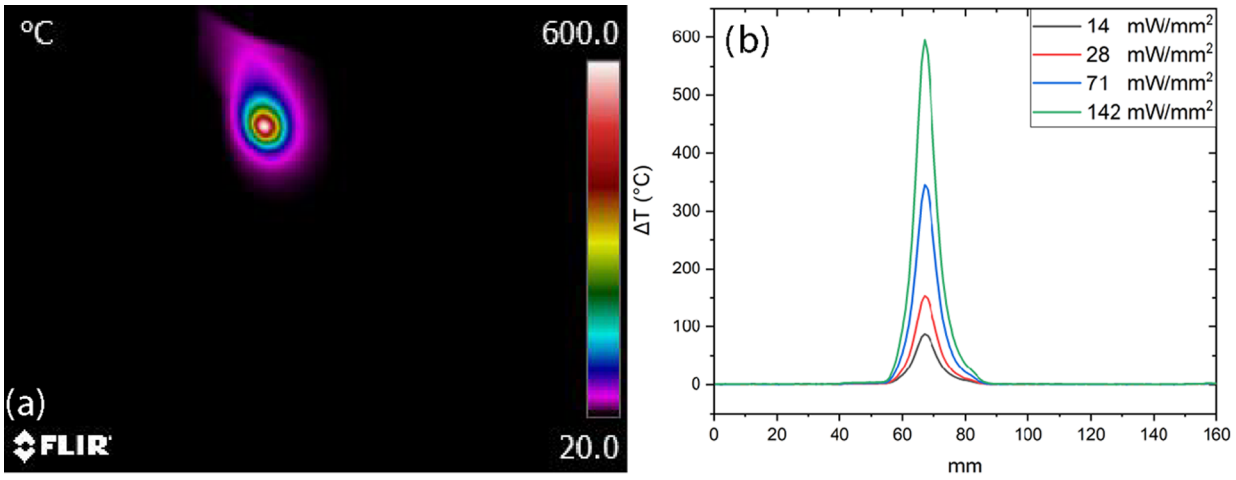

Figure 3. (a) Experimental macroscopic thermal map after 30 s of illumination with a laser intensity of 142 mW/mm^2 and (b) beam profile after 30 s of illumination for the investigated laser intensity.

wavelengths shorter than 900 nm, which corresponds to the absorption edge of amorphous-Si (1.5 eV). In fact, the fabricated SiNWs possess a crystalline core coated by an amorphous shell, as demonstrated in past study.[39]

We finally observe that the light-trapping mechanisms, depending on scattering events, are strongly sensitive to structural parameters (size, size distribution, orientation, and periodicity) of the NW array and have been tailored for several different applications including photovoltaics,[41] surface-enhanced Raman spectroscopy,[30,31,42,43] and photothermal therapy.[27] Here, the randomness in the orientation and size distribution causes a broadening of the frequency range of the scattered light and randomization of the incident light more efficient than in an ordered array of vertical nanowires.[44,45] These features provide further benefits in the light absorption enhancement and conversion in thermal energy.

Photothermal Characterization. The investigation of the thermal response of the SiNW platform was performed utilizing an IR thermocamera (FLIR E60) and a continuous-wave laser source (Coherent, Verdi 5W) with λ = 532 nm at different intensities in the range of 14−142 mW/mm^2. Further details are reported in the Methods section. After switching on the laser, the SiNW temperature rapidly increases (ΔT) as a result of the photothermal conversion, until reaching a stable temperature maximum. The temperature profiles measured for different laser intensities are shown in Figure 2a. ΔT registered for the lowest laser intensity is about 85 °C, while the extremely high value of 595 °C is obtained at a laser intensity of 142 mW/mm^2 (see Figure 2a). As illustrated in Figure 2b, ΔT is quite linearly proportional to the laser power within the considered range. The response time as a function of the laser intensity is reported in Figure 2c. SiNWs exhibit a very fast response, with a rise time (calculated as the time required to reach 90% of the stable ΔT value when the laser is on) of less than 10 s, for the lowest intensity, and about 5 s in the case of 142 mW/mm^2 with a ΔT > 550 °C, as shown by black squares in Figure 2c. It is worth noting that in this case, a remarkable ΔT = 330 °C is reached in only 1 s, further validating the impressive thermal behavior of the proposed nanostructures. The decay time (calculated as the time required to recover within 10% of the initial value when the laser is off) is, instead, independent from the beam intensity, and it lasts for about 10 s, as shown by red circles in Figure 2c. Furthermore, the capability to temporally modulate the thermal signal by switching the laser intensity from 28 mW/mm^2 (low power) to 114 mW/mm^2 (high power) every 10 s was investigated. The recorded video of the photothermal measurement is available in the Supporting information. Figure 2d shows that the thermal signal can oscillate between two different temperature values by just switching the power of the exciting light between low and high levels. During the experiment, the physical properties of NWs remain very stable as confirmed by the maximum and minimum signals being unchanged over five low/high laser power cycles. This remarkable photothermal effect can be ascribed to the light-trapping phenomenon that induces a strong enhancement of the light absorption of the NWs (see Figure 1c) directly hit by the laser spot. On the other hand, for indirect band-gap semiconductors, such as Si, the nonradiative recombination of the photogenerated carriers can occur by involving vibrational energy states via crystal structure defects and trap sites in the band structure,[37] leading to fast photothermal heating of the material. In fact, using the model reported in ref 46, the rate of energy supplied by the laser light (Q_I) is

$$Q_I = I(1 - 10^{-A_\lambda})\eta \tag{1}$$

where I is the laser power, A_λ is the optical absorption in materials, and η is the thermal conversion efficiency.

The balancing of Q_I with the rate of energy dissipated to an external environment (Q_{Ext}) returns

$$\sum_i m_i C_{p,i} \frac{dT}{dt} = Q_I - Q_{Ext} \tag{2}$$

where m_i and $C_{p,i}$ are the mass and heat capacity of the components of the system, respectively, and T and t represent temperature and time, respectively. To visualize the temperature spatial distribution in the SiNWs under laser illumination, in Figure 3a, we report the thermal map, after 30 s of illumination with a laser intensity at 142 mW/mm^2. The image demonstrates that almost all of the photothermal effects are confined around the laser spot. In fact, as highlighted in Figure 3b, the beam profile resembles a Gaussian in all investigated cases, with a full-width at half-maximum (FWHM) between 8.8 and 9.2 mm, which is almost independent of the laser intensity.

https://doi.org/10.1021/acs.jpcc.1c03732
J. Phys. Chem. C 2021, 125, 14134−14140

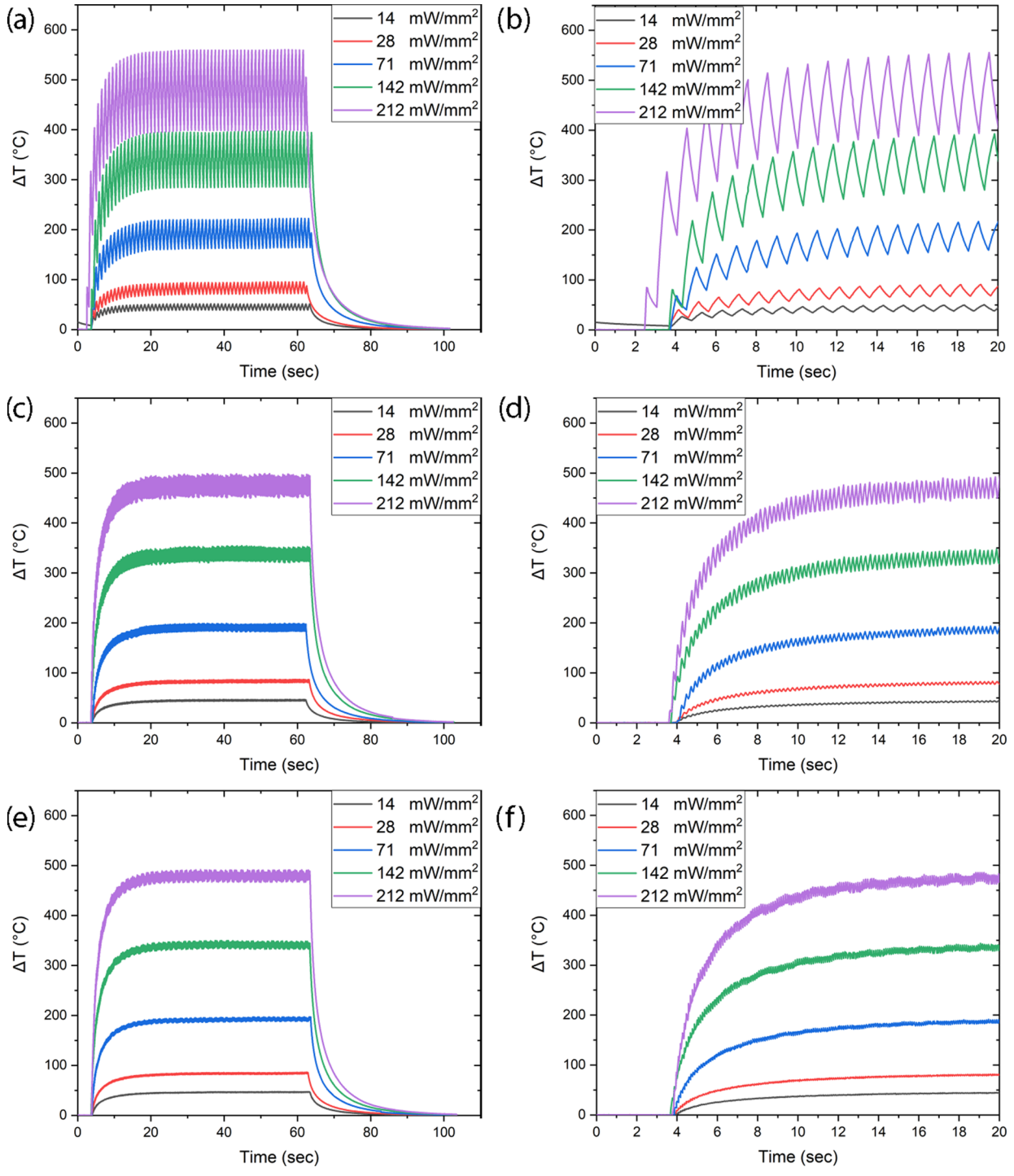

Figure 4. (a) Experimental macroscopic temperature variation of SiNWs at different laser intensities (λ = 532 nm) and chopper frequencies of (a) 1 Hz, (b) zoom of 1 Hz, (c) 5 Hz, (d) zoom of 5 Hz, (e) 10 Hz, and (f) zoom of 10 Hz.

Next, the dynamic thermal response of the proposed NWs was experimentally studied by interrupting the laser beam with a chopper operating at a frequency of 1, 5, and 10 Hz (see Figure 4). In this configuration, the maximum ΔT achieved is almost 40% lower with respect to the above mentioned static case owing to the fact that rapid stopping of the impinging light cannot permit to generate all of the heat that the system can produce. Therefore, the intensity of the laser beam was increased up to 212 mW/mm^2 without saturating the IR camera sensor. Now, the maximum ΔT depends not only on the intensity but also on the chopper frequency. In particular, at 1 Hz, it is possible to reach the extremely high-temperature variation of 150 °C for the highest laser intensity in one period. At a higher chopper frequency, the temperature variation is lower because the time is not enough for the system to generate heat before the laser is interrupted. It is worth noting that at fixed intensity and chopper frequency, the temperature variation is constant, indicating the high responsiveness of the proposed nanowires. The chopper frequency, therefore, provides a novel method to remotely control the temperature

https://doi.org/10.1021/acs.jpcc.1c03732
J. Phys. Chem. C 2021, 125, 14134−14140

variation of a photothermally heated nanosource. In fact, an almost constant ΔT = 45 °C is achieved using 10 Hz and the lowest laser intensity (14 mW/mm^2), enabling application in nanomedicine where low-temperature increments are necessary, whereas high ΔT are more suitable in nanoengineering/metallurgy.

CONCLUSIONS

This work reports on the enhanced photothermal conversion effect observed in disordered SiNWs, arising from the combination of the efficient light trapping in SiNWs and the nonradiative recombination of free carriers. This induces a stable, fast, and localized heat generation and hence an increase in local temperature. The temperature signal is easily controlled under continuous or pulsed laser illumination and can be tuned in a wide range between a few tens up to ≈600 °C. These features together with a low-cost, low-temperature, and large-area fabrication technology make the disordered SiNWs a versatile photothermal platform well suited for multiple applications ranging from nanomedicine, chemistry, and micro-/nanoengineering, which need very different energies to be delivered.

ASSOCIATED CONTENT

Supporting Information

The Supporting Information is available free of charge at https://pubs.acs.org/doi/10.1021/acs.jpcc.1c03732.

Recorded video of the photothermal measurement acquired by switching the laser intensity from 28 mW/mm^2 (low power) to 114 mW/mm^2 (high power) every 10 s (S1 video) (MP4)

AUTHOR INFORMATION

Corresponding Authors

Annalisa Convertino − *Institute for Microelectronics and Microsystems, CNR, I-00133 Rome, Italy;* orcid.org/0000-0002-9426-8352; Email: annalisa.convertino@cnr.it

Roberto Caputo − *Physics Department, University of Calabria, I-87036 Arcavacata di Rende, CS, Italy; CNR Nanotec-Institute of Nanotechnology, I-87036 Rende, CS, Italy; Institute of Fundamental and Frontier Sciences, University of Electronic Science and Technology of China, Chengdu 610054, China;* orcid.org/0000-0002-0065-8422; Email: roberto.caputo@unical.it

Authors

Antonio Ferraro − *Physics Department, University of Calabria, I-87036 Arcavacata di Rende, CS, Italy; CNR Nanotec-Institute of Nanotechnology, I-87036 Rende, CS, Italy;* orcid.org/0000-0003-0189-6729

Pino Cerza − *Physics Department, University of Calabria, I-87036 Arcavacata di Rende, CS, Italy; CNR Nanotec-Institute of Nanotechnology, I-87036 Rende, CS, Italy*

Valentina Mussi − *Institute for Microelectronics and Microsystems, CNR, I-00133 Rome, Italy*

Luca Maiolo − *Institute for Microelectronics and Microsystems, CNR, I-00133 Rome, Italy*

Complete contact information is available at: https://pubs.acs.org/10.1021/acs.jpcc.1c03732

Notes

The authors declare no competing financial interest.

ACKNOWLEDGMENTS

The authors thank the "Area della Ricerca di Roma 2", Tor Vergata, for the access to the ICT Services (ARToV-CNR) for the use of the COMSOL Multiphysics Platform and Origin Lab, and the Infrastructure "BeyondNano" (PONa3-00362) of CNR-Nanotec for the access to research instruments.

REFERENCES

(1) Fei Guo, C.; Sun, T.; Cao, F.; Liu, Q.; Ren, Z. Metallic nanostructures for light trapping in energy-harvesting devices. *Light: Sci. Appl.* **2014**, *3*, No. e161.

(2) Ferraro, A.; Zografopoulos, D. C.; Verschuuren, M. A.; de Boer, D. K.; Kong, F.; Urbach, H. P.; Beccherelli, R.; Caputo, R. Directional Emission of Fluorescent Dye-Doped Dielectric Nanogratings for Lighting Applications. *ACS Appl. Mater. Interfaces* **2018**, *10*, 24750−24757.

(3) Fujimoto, T.; Imai, Y.; Tei, K.; Ito, S.; Kanazawa, H.; Yamaguchi, S. High temperature heat source generation with quasi-continuous wave semiconductor lasers at power levels of 6 W for medical use. *J. Biomed. Opt.* **2014**, *19*, No. 101502.

(4) Lio, G. E.; Ferraro, A.; Giocondo, M.; Caputo, R.; De Luca, A. Color Gamut Behavior in Epsilon Near-Zero Nanocavities during Propagation of Gap Surface Plasmons. *Adv. Opt. Mater.* **2020**, No. 2000487.

(5) Lio, G. E.; Ferraro, A.; Ritacco, T.; Aceti, D. M.; De Luca, A.; Giocondo, M.; Caputo, R. Leveraging on ENZ Metamaterials to Achieve 2D and 3D Hyper-Resolution in Two-Photon Direct Laser Writing. *Adv. Mater.* **2021**, *33*, No. 2008644.

(6) Govorov, A. O.; Richardson, H. H. Generating heat with metal nanoparticles. *Nano Today* **2007**, *2*, 30−38.

(7) Baffou, G.; Quidant, R. Thermo-plasmonics: using metallic nanostructures as nano-sources of heat. *Laser Photonics Rev.* **2013**, *7*, 171−187.

(8) Govorov, A. O.; Zhang, H.; Demir, H. V.; Gun'ko, Y. K. Photogeneration of hot plasmonic electrons with metal nanocrystals: Quantum description and potential applications. *Nano Today* **2014**, *9*, 85−101.

(9) Palermo, G.; Cataldi, U.; Condello, A.; Caputo, R.; Bürgi, T.; Umeton, C.; De Luca, A. Flexible thermo-plasmonics: an opto-mechanical control of the heat generated at the nanoscale. *Nanoscale* **2018**, *10*, 16556−16561.

(10) Jauffred, L.; Samadi, A.; Klingberg, H.; Bendix, P. M.; Oddershede, L. B. Plasmonic heating of nanostructures. *Chem. Rev.* **2019**, *119*, 8087−8130.

(11) Lio, G. E.; Palermo, G.; De Luca, A.; Caputo, R. Tensile control of the thermal flow in plasmonic heaters realized on flexible substrates. *J. Chem. Phys.* **2019**, *151*, No. 244707.

(12) Lio, G. E.; Palermo, G.; Caputo, R.; De Luca, A. Opto-mechanical control of flexible plasmonic materials. *J. Appl. Phys.* **2019**, *125*, No. 082533.

(13) Baffou, G.; Cichos, F.; Quidant, R. Applications and challenges of thermoplasmonics. *Nat. Mater.* **2020**, *19*, 946−958.

(14) Lio, G. E.; De Luca, A.; Umeton, C. P.; Caputo, R. Opto-mechanically induced thermoplasmonic response of unclonable flexible tags with hotspot fingerprint. *J. Appl. Phys.* **2020**, *128*, No. 093107.

(15) Ferraro, A.; Lio, G. E.; Hmina, A.; Palermo, G.; Maurer, T.; Caputo, R. Tailoring of Plasmonic Functionalized Metastructures to Enhance Local Heating Release, arXiv:2105.09135. arXiv.org e-Print archive. https://arxiv.org/abs/2105.09135 (submitted May 19, 2021).

(16) Jaque, D.; Maestro, L. M.; Del Rosal, B.; Haro-Gonzalez, P.; Benayas, A.; Plaza, J.; Rodriguez, E. M.; Sole, J. G. Nanoparticles for photothermal therapies. *Nanoscale* **2014**, *6*, 9494−9530.

(17) Wang, Z.; Tao, P.; Liu, Y.; Xu, H.; Ye, Q.; Hu, H.; Song, C.; Chen, Z.; Shang, W.; Deng, T. Rapid charging of thermal energy storage materials through plasmonic heating. *Sci. Rep.* **2014**, *4*, No. 6246.

(18) Benndorf, K. Multiple levels of native cardiac Na+ channels at elevated temperature measured with high-bandwidth/low-noise patch clamp. *Pflügers Arch.* **1993**, *422*, 506−515.
(19) DeCoursey, T. E.; Cherny, V. V. Temperature dependence of voltage-gated H+ currents in human neutrophils, rat alveolar epithelial cells, and mammalian phagocytes. *J. Gen. Physiol.* **1998**, *112*, 503−522.
(20) Huang, H.; Delikanli, S.; Zeng, H.; Ferkey, D. M.; Pralle, A. Remote control of ion channels and neurons through magnetic-field heating of nanoparticles. *Nat. Nanotechnol.* **2010**, *5*, 602−606.
(21) David, G.; Barrett, E. F. Stimulation-evoked increases in cytosolic [Ca2+] in mouse motor nerve terminals are limited by mitochondrial uptake and are temperature-dependent. *J. Neurosci.* **2000**, *20*, 7290−7296.
(22) Plaksin, M.; Shapira, E.; Kimmel, E.; Shoham, S. Thermal transients excite neurons through universal intramembrane mechanoelectrical effects. *Phys. Rev. X* **2018**, *8*, No. 011043.
(23) Martino, N.; Feyen, P.; Porro, M.; Bossio, C.; Zucchetti, E.; Ghezzi, D.; Benfenati, F.; Lanzani, G.; Antognazza, M. R. Photothermal cellular stimulation in functional bio-polymer interfaces. *Sci. Rep.* **2015**, *5*, No. 8911.
(24) Farah, N.; Zoubi, A.; Matar, S.; Golan, L.; Marom, A.; Butson, C. R.; Brosh, I.; Shoham, S. Holographically patterned activation using photo-absorber induced neural-thermal stimulation. *J. Neural Eng.* **2013**, *10*, No. 056004.
(25) Tode, J.; Richert, E.; Koinzer, S.; Klettner, A.; von der Burchard, C.; Brinkmann, R.; Lucius, R.; Roider, J. Thermal stimulation of the retina reduces Bruchas membrane thickness in age related macular degeneration mouse models. *Transl. Vis. Sci. Technol.* **2018**, *7*, No. 2.
(26) Wang, C.; Yin, L.; Zhang, L.; Xiang, D.; Gao, R. Metal oxide gas sensors: sensitivity and influencing factors. *Sensors* **2010**, *10*, 2088−2106.
(27) Semancik, S.; Cavicchi, R. E.; Wheeler, M.; Tiffany, J.; Poirier, G.; Walton, R.; Suehle, J. S.; Panchapakesan, B.; DeVoe, D. Microhotplate platforms for chemical sensor research. *Sens. Actuators, B* **2001**, *77*, 579−591.
(28) Convertino, A.; Mussi, V.; Maiolo, L.; Ledda, M.; Lolli, M. G.; Bovino, F. A.; Fortunato, G.; Rocchia, M.; Lisi, A. Array of disordered silicon nanowires coated by a gold film for combined NIR photothermal treatment of cancer cells and Raman monitoring of the process evolution. *Nanotechnology* **2018**, *29*, No. 415102.
(29) Saracino, E.; Maiolo, L.; Polese, D.; Semprini, M.; Borrachero-Conejo, A. I.; Gasparetto, J.; Murtagh, S.; Sola, M.; Tomasi, L.; Valle, F.; et al. A Glial-Silicon Nanowire Electrode Junction Enabling Differentiation and Noninvasive Recording of Slow Oscillations from Primary Astrocytes. *Adv. Biosyst.* **2020**, *4*, No. 1900264.
(30) Maiolo, L.; Polese, D.; Pecora, A.; Fortunato, G.; Shacham-Diamand, Y.; Convertino, A. Highly disordered array of silicon nanowires: an effective and scalable approach for performing and flexible electrochemical biosensors. *Adv. Healthcare Mater.* **2016**, *5*, 575−583.
(31) Convertino, A.; Mussi, V.; Maiolo, L. Disordered array of Au covered Silicon nanowires for SERS biosensing combined with electrochemical detection. *Sci. Rep.* **2016**, *6*, No. 25099.
(32) Paria, D.; Convertino, A.; Mussi, V.; Maiolo, L.; Barman, I. Silver-Coated Disordered Silicon Nanowires Provide Highly Sensitive Label-Free Glycated Albumin Detection through Molecular Trapping and Plasmonic Hotspot Formation. *Adv. Healthcare Mater.* **2020**, *10*, No. 2001110.
(33) Mussi, V.; Ledda, M.; Polese, D.; Maiolo, L.; Paria, D.; Barman, I.; Lolli, M. G.; Lisi, A.; Convertino, A. Silver-coated silicon nanowire platform discriminates genomic DNA from normal and malignant human epithelial cells using label-free Raman spectroscopy. *Mater. Sci. Eng., C* **2021**, *122*, No. 111951.
(34) Cuscunà, M.; Convertino, A.; Zampetti, E.; Macagnano, A.; Pecora, A.; Fortunato, G.; Felisari, L.; Nicotra, G.; Spinella, C.; Martelli, F. On-chip fabrication of ultrasensitive NO2 sensors based on silicon nanowires. *Appl. Phys. Lett.* **2012**, *101*, No. 103101.
(35) Convertino, A.; Cuscuna, M.; Martelli, F. Optical reflectivity from highly disordered Si nanowire films. *Nanotechnology* **2010**, *21*, No. 355701.
(36) Street, R.; Qi, P.; Lujan, R.; Wong, W. Reflectivity of disordered silicon nanowires. *Appl. Phys. Lett.* **2008**, *93*, No. 163109.
(37) Gärtner, W. W. Photothermal effect in semiconductors. *Phys. Rev.* **1961**, *122*, No. 419.
(38) Cuscunà, M.; Convertino, A.; Mariucci, L.; Fortunato, G.; Felisari, L.; Nicotra, G.; Spinella, C.; Pecora, A.; Martelli, F. Low-temperature, self-catalyzed growth of Si nanowires. *Nanotechnology* **2010**, *21*, No. 255601.
(39) Convertino, A.; Cuscunà, M.; Nicotra, G.; Spinella, C.; Felisari, L.; Fortunato, G.; Martelli, F. Low-temperature growth of In-assisted silicon nanowires. *J. Cryst. Growth* **2011**, *335*, 10−16.
(40) Pimentel-Domínguez, R.; Moreno-Álvarez, P.; Hautefeuille, M.; Chavarría, A.; Hernández-Cordero, J. Photothermal lesions in soft tissue induced by optical fiber microheaters. *Biomed. Opt. Express* **2016**, *7*, 1138−1148.
(41) Peng, K.; Xu, Y.; Wu, Y.; Yan, Y.; Lee, S.-T.; Zhu, J. Aligned single-crystalline Si nanowire arrays for photovoltaic applications. *Small* **2005**, *1*, 1062−1067.
(42) Zhang, C.; Siddhanta, S.; Paria, D.; Li, Y.; Zheng, C.; Barman, I. Spectroscopy-Assisted Label-free Molecular Analysis of Live Cell Surface with Vertically Aligned Plasmonic Nanopillars. *Small* **2021**, *17*, No. 2100161.
(43) Convertino, A.; Cuscuna, M.; Martelli, F.; Manera, M. G.; Rella, R. Silica nanowires decorated with metal nanoparticles for refractive index sensors: three-dimensional metal arrays and light trapping at plasmonic resonances. *J. Phys. Chem. C* **2014**, *118*, 685−690.
(44) Muskens, O. L.; Diedenhofen, S. L.; Kaas, B. C.; Algra, R. E.; Bakkers, E. P.; Gomez Rivas, J.; Lagendijk, A. Large photonic strength of highly tunable resonant nanowire materials. *Nano Lett.* **2009**, *9*, 930−934.
(45) Bao, H.; Ruan, X. Optical absorption enhancement in disordered vertical silicon nanowire arrays for photovoltaic applications. *Opt. Lett.* **2010**, *35*, 3378−3380.
(46) Richardson, H. H.; Carlson, M. T.; Tandler, P. J.; Hernandez, P.; Govorov, A. O. Experimental and theoretical studies of light-to-heat conversion and collective heating effects in metal nanoparticle solutions. *Nano Lett.* **2009**, *9*, 1139−1146.

https://doi.org/10.1021/acs.jpcc.1c03732
J. Phys. Chem. C 2021, 125, 14134−14140